

Progressive evolution of tunneling characteristics of *in situ* fabricated intrinsic Josephson junctions in $\text{Bi}_2\text{Sr}_2\text{CaCu}_2\text{O}_{8+\delta}$ single crystals

Yong-Joo Doh, Hu-Jong Lee, and Hyun-Sik Chang

Department of Physics, Pohang University of Science and Technology, Pohang 790-784, Republic of Korea

(Received 26 April 1999; revised manuscript received 7 September 1999)

Stacks of a few intrinsic tunnel junctions were microfabricated on the surface of $\text{Bi}_2\text{Sr}_2\text{CaCu}_2\text{O}_{8+\delta}$ single crystals. The number of junctions in a stack was tailored by progressively increasing the height of the stack by ion-beam etching, while its tunneling characteristics were measured *in situ* in a vacuum chamber for temperatures down to ~ 13 K. Using this *in situ* etching/measurements technique in a single piece of crystal, we systematically excluded any spurious effects arising from variations in the junction parameters and made clear analysis on the following properties of the surface and inner conducting planes. First, the tunneling resistance and the current-voltage curves are scaled by the surface junction resistance. Second, we confirm that the reduction in both the gap and the superconducting transition temperature of the surface conducting plane in contact with a normal metal is not caused by the variation in the doping level, but is caused by the proximity contact. Finally, the main feature of a junction is not affected by the presence of other junctions in a stack in a low-bias region.

I. INTRODUCTION

Recently both superconducting and normal-state tunneling characteristics of junctions intrinsically formed in crystals of extremely anisotropic high- T_c materials such as $\text{Bi}_2\text{Sr}_2\text{CaCu}_2\text{O}_{8+\delta}$ (Bi-2212) and $\text{Tl}_2\text{Ba}_2\text{Ca}_2\text{Cu}_3\text{O}_{10+\delta}$ (Tl-2223) have attracted much research attention.¹⁻²⁹ Previous experimental investigations by many groups have revealed that the superconducting order parameter in the crystals is periodically modulated along the c axis and the interlayer coupling at low-enough temperatures has a Josephson nature. Existence of such naturally formed intrinsic Josephson junctions has been directly confirmed by c -axis tunneling measurements, using small-sized stacks or mesa structures on the surface of single crystals, including current-voltage (IV) characteristics,²⁻¹² temperature or magnetic-field dependence of the critical current,¹³⁻¹⁸ dynamics of Josephson vortices,¹⁹⁻²³ microwave responses,²⁴⁻²⁶ and the Josephson microwave emission.²⁷

Electron-tunneling spectroscopy has been conceived as one of the most powerful means to determine superconducting gap and its anisotropy.³⁰⁻³⁶ Compared to other spectroscopic techniques,³⁷⁻³⁹ electron-tunneling spectroscopy has a very high energy resolution of the electronic structure near the Fermi level E_F . Tunneling spectroscopy and its interpretation on high- T_c materials using conventional techniques such as scanning tunneling spectroscopy, however, have often been controversial, due to problems of poor surface characterizations mainly arising from an extremely short coherence length and uncertainty in the transverse momentum direction of the particles upon tunneling via a small tip.^{32,33} These problems have been conveniently circumvented by a tunneling study using intrinsic junctions (IJ's) in high- T_c materials. Especially, tunneling measurements on a small-sized stack, including only a few intrinsic junctions, provide valuable information on the nature of the inherent superconducting gap and the pairing mechanism of unusual symmetry in the materials.

It is unsettled yet, however, whether the individual junctions in a stack behave independently or are correlated with each other. Junctions in a stack could be inductively coupled by supercurrents flowing on thin conducting planes^{19,42} or coupled by the charging of thin conducting planes by tunneling electrons.⁴³ Thus the plasma oscillations excited in a stack of intrinsic junctions, for example, show collective modes.^{2,25} However, some previous studies indicate the opposite may be true. For dc bias current applied along the c axis, coupling between adjacent junctions is small enough so that each junction can be assumed to be independent.^{5,9} Correlated junction behavior would affect the usefulness of a stack for device applications. For instance, correlated junction behavior is useful for high-frequency oscillator applications but detrimental to voltage standards applications.²⁵ Thus, the issue of correlation of the tunneling characteristics of intrinsic junctions still remains of prime concern from both academic and device-application points of view.

Tunneling spectroscopy on the surface of high- T_c materials is widely used to probe the nature of order-parameter symmetry, mostly using hybrid junctions consisting of conventional and high- T_c superconducting electrodes.^{29,44,45} In this case, it is utterly important to make sure that the superconducting properties of the surface layer, such as the transition temperature, the gap value, and its order-parameter symmetry, do not deviate from those of inherent bulk properties.⁴⁶ Recently, surface-sensitive spectroscopy such as angle-resolved photoemission spectroscopy,³⁸ scanning tunneling spectroscopy,^{34,35} break-junction tunneling,³⁶ and intrinsic-junction tunneling,^{28,40,41} is increasingly used to investigate the in-plane normal-state conducting properties of high- T_c materials, i.e., the existence and nature of the pseudogap, especially as varying the doping level. Since the size of the pseudogap is known to be sensitive to the doping level in the underdoped regime,³⁴⁻³⁶ any possible significant oxygen deficiency in the surface layer would lead to a very serious misinterpretation of the intrinsic bulk properties of

the conducting planes. Additionally, our previous study¹¹ indicates that depositing noble-metal film such as Au on the surface of high- T_c materials, often used for surface protection for electron conduction measurements, causes a suppression of the surface layer's superconductivity by its proximity contact to normal metal. In this respect, it is of prime importance to probe any variation in the doping level of the surface layer from that of the inner layers with intrinsic bulk properties.

Most studies on the intrinsic tunneling effect in high- T_c superconductors, both in superconducting and normal states, have been done to date by fabricating a small elevated stack structure (with the cross-sectional area usually of a few hundreds μm^2) on the surface of single crystals with a few IJ's in it. The number of the junctions in a stack is varied by changing the height of the stack during the fabrication process using ion-beam etching or chemical wet etching. In this way, however, accurate tailoring of the number of junctions is a difficult task. To get a deeper understanding of the interlayer coupling characteristics of an individual intrinsic junction as well as the conducting properties in a plane, both in superconducting and normal states, careful *in situ* control of the number of IJ's in a stack is required while monitoring their tunneling characteristics.⁸

In this report, we first examine the possibility of any significant variation of the doping level in the surface layer of high- T_c single crystals in contact with normal metals, along with a change in the superconducting properties. We then discuss the physical implication of the scaling of tunneling resistance and the IV curves with respect to surface junction resistance. We also examine whether the main feature of a junction is influenced by the presence of other junctions in a stack. To that end, we focus on the evolution of the tunneling characteristics of IJ's while progressively increasing the number of junctions in a stack fabricated on the surface of Bi-2212 single crystals. Ion-beam etching was used in combination with *in situ* cryogenic measurements, similar to the technique reported in Ref. 8. The number of IJ's in a stack was increased in sequence by carefully controlling the low-energy ion-beam etching time with preformed metallic electrodes on the surface of the stack. Between each etching stage the c -axis tunneling IV characteristics and the temperature dependence of the c -axis tunneling resistance $R_c(T)$ were taken while varying the substrate temperature from room temperature down to ~ 13 K.

This study directly confirms our previous finding that a weak junction (WJ) forms at the surface of a Bi-2212 stack¹¹ that is in contact with a normal-metal electrode. The *in situ* etching/measurements technique confirms that the suppression of the gap and the transition temperature in the surface layer of a stack does not result from the change in the doping level or from the proximity-induced weak superconductivity in the Bi-O layer^{5,6} that may be surfaced. Rather, the suppression results presumably from the proximity contact of the surface layer with $d_{x^2-y^2}$ symmetry to the Au normal metal. This study also convincingly demonstrates that the individual junction is little influenced by the presence of other junctions in a stack in a low-bias region. As to the cause of development of negative dynamic resistance in the high-bias region of the IV curves with increasing number of

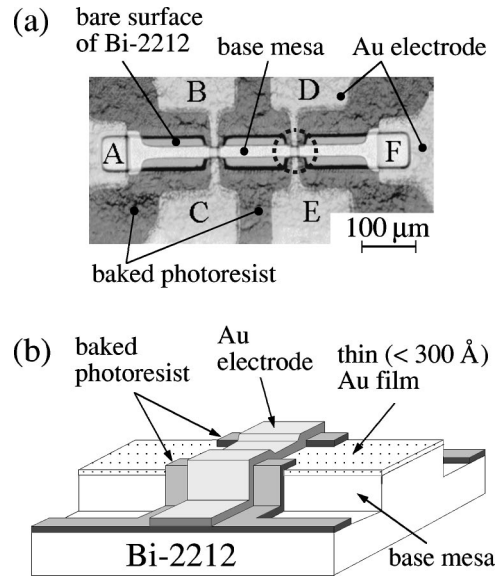


FIG. 1. (a) An optical micrograph of a sample prior to *in situ* ion-beam etching. Four small stacks were fabricated on the top surface of the base mesa. A-F denote the Au electrodes. Data are reported for the configuration, where A and D (B and F) were used for biasing currents and E and F(A and C) for voltage measurements. (b) Enlarged schematic view of the dashed-circle region in (a).

junctions in a stack, we find that the Joule heating effect, not the nonequilibrium, can be a good candidate for that cause.

II. EXPERIMENTS

Bi-2212 crystals were grown from a melt using alumina crucibles, details of which are described elsewhere.⁴⁷ Pieces of single-crystal platelets with typical size $\sim 0.8 \times 0.4 \times 0.03$ mm³ were selected from a mass of the cooled melt. A platelet was glued onto a sapphire substrate by negative photoresist, then hard-baked. An optically smooth surface was prepared by cleaving a platelet of single crystal using Scotch tape. Right after cleaving, a 1000-Å-thick Au film was deposited on the surface of the Bi-2212 crystals to protect the surface from any contamination during stack-fabrication processes.

We then patterned a large “base mesa” of size $\sim 450 \times 15 \times 1$ μm^3 on the crystal surface, using standard photolithography and Ar-ion-beam etching, with beam voltage and current density $V_{beam} = 300$ V and $I_{beam} = 0.8$ mA/cm², respectively. Any residue of burned-out photoresist on the crystal surface was stripped off by oxygen-plasma etching. Then a patterned layer of photoresist was placed around the base mesa and hard baked to insulate the region, excluding the top surface of the base mesa. A thick Au film (~ 8000 Å) was deposited,⁴⁸ and connection pads from the base mesa were patterned and ion-beam etched. Thereafter, the electric pads of Au (totally ~ 9000 Å) crossing the base mesa acted as masks for the small stacks in the further *in situ* etching process. In this stage, a thin (less than 300 Å in nominal thickness) Au film was intentionally left on the top surface of the base mesa between the pads to prevent the inadvertent premature formation of small stack structures. The remaining Au film would be removed during the next *in situ* measurement process with controlled ion-beam etching.

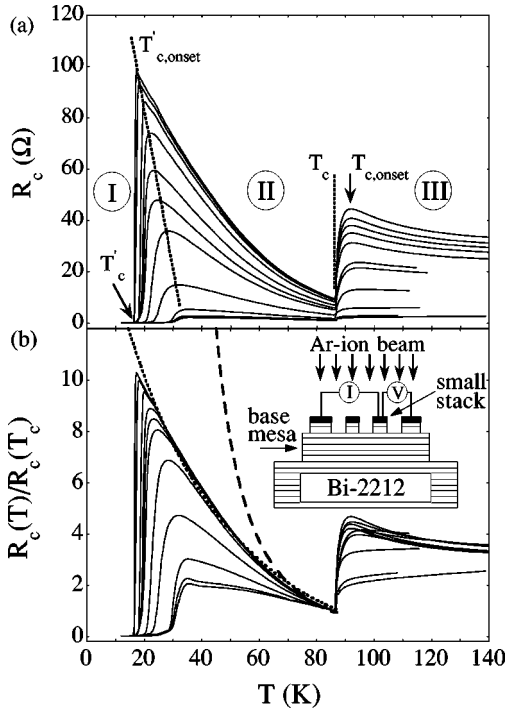


FIG. 2. (a) Progressive evolution of the c -axis resistance $R_c(T)$ curves with increasing etching times; $t_e = 0, 3, 5, 6.5, 10, 12, 15, 19, 22, 26,$ and 30 min from bottom to top. The contact resistance was not subtracted. The characteristic temperatures T'_c , $T'_{c,onset}$, T_c , and $T_{c,onset}$ and the temperature regions I, II, III are defined in the text. The dotted lines show the t_e dependence of T_c and $T'_{c,onset}$. (b) A replot of the $R_c(T)$ curves, where $R_c(T)$ was rescaled by $R_c(T_c = 86.5 \text{ K})$. The dotted line is a fit to Eq.(2) for a single normal-metal/insulator/ d -wave-superconductor ($N'ID$) surface junction with $\Delta_0 = 32.6 \text{ meV}$, in comparison with a fit (dashed line) with s -wave gap $\Delta_0 = 17 \text{ meV}$. Inset: a schematic view of the configuration for the *in situ* three-terminal measurements.

Figure 1 illustrates the optical photograph and the corresponding schematic view of a specimen after completing the whole process prior to the *in situ* etching.

For *in situ* monitoring of the tunneling characteristics of a small stack, the specimen was loaded into an ultrahigh-vacuum chamber equipped with a liquid-helium cooling pot as well as an ion-beam etching system. Ion-beam etching and cryogenic measurements could be repeated without breaking the vacuum. The remnant 300-\AA -thick Au film and Bi-2212 crystal underneath were further etched, while forming four small stacks on the base mesa. The junction size was defined by the width ($\sim 15 \mu\text{m}$) of the base mesa and ($\sim 12 \mu\text{m}$) of the electrical pads overlaid perpendicularly to the length of the base mesa. In this etching stage we used sufficiently low ion-beam voltage ($V_{beam} = 100 \text{ V}$) and current density ($I_{beam} = 0.16 \text{ mA/cm}^2$) to enhance the controllability of the etching rate. The height of a small stack was controlled by the total etching time t_e . In every 1–2-min etching, the chamber was pumped out and a stack was characterized in a three-probe-measurement configuration [see the inset in Fig. 2(b)]. The $R_c(T)$ was measured using a dc method with a constant-bias current of $10 \mu\text{A}$. To reduce the effect of external noise, low-pass filters were connected to the voltage and the current leads. A recent report²⁹ indicates that, using the similar cleaving technique on Bi-2212 crystals, step

structures with a height of one-half unit cell usually forms in the samples in an area of $30 \times 30 \mu\text{m}^2$. We did not observe any evidence for the existence of a step in our tunneling results. In this study, we took measurements for three different stacks, all showing similar features. We present a typical set of data obtained from one of the specimens.

III. RESULTS AND DISCUSSION

A. $R_c(T)$ curves

Progressive evolution of $R_c(T)$ by increasing the *in situ* etching time t_e up to 30 min is presented in Fig. 2(a). Increment of the number of junctions in the stack with increasing t_e was monitored by counting the number of quasiparticle branches in the corresponding IV curves. Figure 2(a) reveals that when we lower the temperature from room temperature down to the bulk superconducting transition temperature, the $R_c(T)$ curves show metallic behavior at $t_e \leq 5 \text{ min}$ but gains a slightly semiconducting behavior at $t_e \geq 6.5 \text{ min}$ where the value of R_c reaches a maximum at $T_{c,onset}$ ($\approx 92 \text{ K}$). The value of R_c then starts dropping abruptly and reaches a minimum at T_c ($\approx 86.5 \text{ K}$). Interestingly, for all the values of t_e , R_c remains finite below T_c and gradually increases again up to the secondary resistance maximum at $T'_{c,onset}$. In the range of $T'_{c,onset} < T < T_c$ the temperature dependence of R_c shows a more pronounced semiconducting behavior. Below $T'_{c,onset}$ the value of R_c drops sharply, especially for high values of t_e , and vanishes to 0.1Ω at T'_c ($\approx 15 \text{ K}$) and below.

As t_e increases, $T'_{c,onset}$ decreases from $\sim 36 \text{ K}$ to $\sim 17 \text{ K}$, as denoted by the dotted guideline in Fig. 2(a). All other characteristic temperatures, $T_{c,onset}$, T_c , and T'_c , however, remain almost insensitive to the etching time. The transition width $\Delta T'_c$ ($\approx 0.3\text{--}5.0 \text{ K}$) near T'_c gets sharper with increasing t_e , while ΔT_c ($\approx 2.3 \text{ K}$) near T_c remains unchanged. The behavior of $R_c(T)$ near $T'_{c,onset}$ is not only sensitive to t_e , but is also highly affected by the ambient condition. For instance, the peak value of $R_c(T'_{c,onset})$ increases rapidly and T'_c is suppressed significantly for rf irradiation of power level as low as -30 dBm (not shown). $R_c(T)$ near $T'_{c,onset}$ is so sensitive to the rf noise that the data taken without filters are greatly affected.

For the sake of clarity we divide the temperature range into three regions: Region I ($T < T'_{c,onset}$), II ($T'_{c,onset} < T < T_c$), and III ($T > T_c$), as shown in Fig. 2(a). The total number of quasiparticle branches obtained from the IV curves in Region I for the corresponding etching times are $n = 4$ ($t_e = 6.5 \text{ min}$), 4 (8 min), 5 (10 min), 5 (12 min), 6 (15 min), 8 (19 min), 9 (22 min), 10 (26 min), and 12 (30 min).

In Region I, the stack has $\text{Au}/D'/IDIDID\dots$ configuration, where $D(D')$ denotes the (suppressed) superconducting layer with $d_{x^2-y^2}$ symmetry. Since both the surface and inner junctions are Josephson coupled the junction resistance subtracts from the value of R_c for a low current bias.⁴⁹ Thus, R_c in this case is essentially the contact resistance R_{CT} between the Au electrode and the surface layer D' ; $R_c(T) = R_{CT} \approx 0.1 \Omega$, which is at least two orders of magnitude smaller than R_c in other temperature ranges.

The finite value of R_c found in the stack in Region II is known to be always present in a three-terminal measurement.^{3,5,11,17,26} Since the IJ's in the stack below T_c should be in zero-resistance state for a low-bias current, the finite R_c at temperatures in Region II in this three-terminal configuration is attributed to the *surface* weak junction consisting of the topmost Cu-O bilayer in the normal state, and the adjacent inner Cu-O bilayer in the superconducting state.¹¹ In other words, the surface Cu-O bilayer underneath the normal-metal electrode has a suppressed transition temperature, which is essentially $T'_{c,onset}$. Thus, in Region II, the configuration becomes Au/N'IDIDID..., where N' denotes the surface layer in its normal state. The corresponding resistance is

$$R_c(T) = R_{CT} + R_{N'ID}(T) \approx R_{N'ID}(T) \quad (1)$$

$$R_{N'ID}(T) = \left[\lim_{V \rightarrow 0} \frac{dI}{dV} \right]^{-1} = \left\{ \lim_{V \rightarrow 0} \frac{d}{dV} \frac{1}{eR'_n} \int_{-\infty}^{\infty} N(E, \Delta) \times [f(E) - f(E + eV)] dE \right\}^{-1}, \quad (2)$$

where $R_{N'ID}(T)$ is the quasiparticle tunneling resistance of the N'ID surface junction or WJ, R'_n its junction resistance, and $f(E)$ the Fermi distribution function. The normalized density of states $N(E, \Delta)$ of the superconducting Cu-O bilayer with $d_{x^2-y^2}$ symmetry can be obtained by averaging over the in-plane angle in k space as⁵⁰ $N(E, \Delta) = \text{Re}[(1/2\pi) \int_0^{2\pi} \{E/\sqrt{E^2 - [\Delta \cos(2\phi)]^2}\} d\phi]$. Here, Δ is the temperature-dependent energy gap of the inner layers.

In Region III, the configuration is Au/N'ININ..., with the tunneling resistance $R_c(T) = R_{CT} + R_{N'IN}(T) + m \times R_{NIN}(T) \approx R_{N'IN}(T) + m \times R_{NIN}(T)$, where N denotes the inner Cu-O bilayer in its normal state, m the total number of IJ's (note that $m = n - 1$), and $R_{N'IN}$ (R_{NIN}) stands for the quasiparticle tunneling resistance of each N'IN (NIN) junction.

From Eqs. (1) and (2) we note that $R_c(T_c) \approx R_{N'ID}(T_c) = R'_n$ and the value increases gradually with increasing t_e . The values of $R_c(T_c)$ in Fig. 2(a) are 1.1, 1.2, 1.8, 3.2, 5.2, 6.0, 7.0, 8.3, 9.0, 9.3, and 9.5 Ω for t_e from 0 up to 30 min [see Fig. 7(a)]. We presume the variation of $R_c(T_c)$ is due to shrinking of the junction area as the etching gets longer, the reason for which will be discussed below.

To study the intrinsic properties of the interlayer coupling or the conduction in the Cu-O planes, one needs to eliminate the effect of the variation in the junction area by normalizing $R_c(T)$ with respect to the junction resistance. Rescaled curve $R_c(T)/R_c(T_c)$ for each set of curves in Fig. 2(a) corresponding to t_e equal to 10 min or longer tends to merge into a single curve at temperatures in Region II [see Fig. 2(b)]. The temperature dependence of the curve is well in accordance with $R_{N'ID}(T)$ expressed in Eq. (2). Note that in Eq. (2) only R'_n has t_e dependence, thus $R_{N'ID}/R'_n$ or equivalently $R_c(T)/R_c(T_c)$ as plotted in Fig. 2(b) should be independent of t_e . The best fit denoted as the dotted curve is obtained for $\Delta_0 \equiv \Delta(0) = 32.6$ meV with the assumption of the BCS-type temperature dependence of the gap,⁵¹ $\Delta(T) = \Delta_0 \tanh(\alpha\sqrt{T_c/T - 1})$ with $\alpha = 1.45$. Although $\alpha = 1.74$ is

valid for the true BCS-type behavior, for this $d_{x^2-y^2}$ symmetry $\alpha = 1.45$ gives a better fit and is consistent with the theoretical prediction.⁵⁰ The fit turns out very satisfactory in almost all temperatures in Region II. The value of Δ_0 is in good agreement with the results of other studies, obtained from *IV* curves of the inner IJ's with DID-junction configurations near the liquid-helium temperature,^{3,9,10} the scanning tunneling spectroscopy,³²⁻³⁵ or photoemission spectroscopy,³⁹ using optimally or slightly overdoped samples.

For comparison, we also draw the best-fit curve with an isotropic *s*-wave gap⁵² with $\Delta_0 = 17$ meV (the dashed curve) which gives, however, only a marginal fit at best near T_c . Any larger *s*-wave gap Δ_0 would result in even a poorer fit over the range of Region II. Insensitivity of the rescaled $R_c(T)$ to the number of IJ's in a stack in Region II indicates that the variation of $R_c(T)$, at least for $t_e \geq 10$ min, was caused by the variation in the junction area with etching. Note that this insensitivity also implies the number of the N'ID junctions does not change with progressive etching; only one N'ID junction exists presumably on the surface of the stack. The deviation of $R_c(T)$ from the merging curve for $t_e < 10$ min is due to an incomplete formation of the stack and will be discussed below. One notices in Fig. 2(b) that the curves $R_c(T)/R_c(T_c)$ do not show any merging behavior in Region III, even for long etching times $t_e > 10$ min. This is consistent with the fact that the $R_c(T)$ in Region III include the tunneling resistances of both number of inner IJ's and the surface WJ, which are scaled by R_n and R'_n [$= R_c(T_c)$], respectively. Thus, $R_c(T)$ in Region III is not scaled by $R_c(T_c)$ alone.

The inset of Fig. 3 shows more details of $R_c(T)$ curves in Region III for $t_e = 15, 19, 22, 26,$ and 30 min corresponding to $n = 6, 8, 9, 10,$ and 12 , respectively. Each curve shows a pronounced metallic behavior in the high-temperature region, which may imply that the conducting planes are in a highly *overdoped* regime,^{17,40,41} gradually turning into a semiconducting behavior around $T = 170 \sim 180$ K with lowering temperatures. Increasing t_e tends to increase $R_c(T)$ in proportion as more IJ's are included in the stack. In Fig. 3 we plot the single junction contribution to the tunneling resistivity $\rho_{c,single}$ as converted from the relation⁸ $R_{c,single}(T) = [R_c(T, i+j) - R_c(T, i)]/j$ using the geometric parameters, the junction area $S = 12 \times 15 \mu\text{m}^2$ and its thickness $d = 12 \text{ \AA}$, for the number of junctions $i+j = 8, 9, 12, 12$ and $i = 6, 6, 8, 6$, respectively. Thus, the curves correspond to averaging *c*-axis resistivity over 2, 3, 4, and 6 junctions, respectively. Since $R_c(T_c)$ as seen in Fig. 2(a) is stabilized for $t_e \geq 15$ min, not much relative error is assumed to be involved in this conversion. Note that the surface WJ contribution is subtracted from $\rho_{c,single}$ and it contains only the inner IJ contribution. One noticeable feature of $\rho_{c,single}$ is that the linear- T behavior is significantly diminished in the temperature range of $T > 170$ K, which implies that the linear- T behavior in the inset of Fig. 3 arises mainly from the surface WJ. The temperature dependence of $\rho_{c,single}$ for different etching stages merges well into a single curve. The dashed curve shows the least χ^2 fit of the data to the empirical relation $\rho_c(T) = (a/T)\exp(\Delta^*/T) + bT + c$ as adopted in Ref. 41 anticipating the occurrence of a pseudogap above

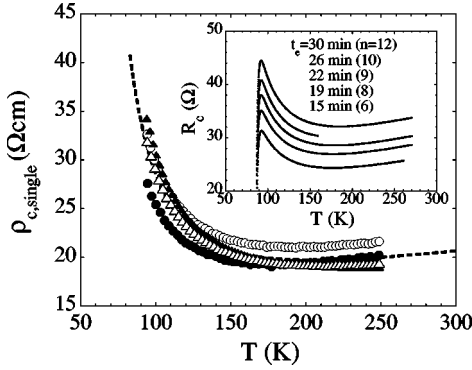


FIG. 3. The single junction contribution to the tunneling resistivity $\rho_{c,single}(T)$ as converted from the relation $R_{c,single}(T) = [R_c(T, i+j) - R_c(T, i)]/j$ and the geometry parameters for $i+j = 8, 9, 12, 12$ and $i = 6, 6, 8, 6$, respectively. Inset: the $R_c(T)$ curves above T_c for $t_e = 15, 19, 22, 26$, and 30 min, corresponding to $n = 6, 8, 9, 10$, and 12 , the total number of quasiparticle branches below T'_c .

T_c , with the best fit parameters of $a = 146 \pm 8 \text{ } \Omega \text{ cm K}$, $\Delta^* = 240 \pm 10 \text{ K}$, $b = 0.0250 \pm 0.008 \text{ } \Omega \text{ cm/K}$, and $c = 17.3 \pm 1.0 \text{ } \Omega \text{ cm}$. The parameter values, especially the value of b , in comparison with Fig. 4 of Ref. 41 indicate that, although the linear- T dependence is much reduced, the inner stacks are still in a overdoped regime. The surface layer, at least with Au protection on it, *cannot be less doped* than the inner layers. Thus, the suppressed superconductivity in the surface layer should be attributed to other causes rather than its oxygen loss. The plausible cause is the effect of the proximity contact of the surface layer with the normal-metal (Au) electrode, as proposed previously.¹¹

B. Tunneling IV curves

Figure 4 shows the evolution of the quasiparticle branches in the tunneling IV curves below T'_c as the stack forms with increasing etching time t_e . In Fig. 4(a), for $t_e = 6.5$ min, one sees four branches develop. As the bias current is increased voltage jumps to an adjacent higher-voltage branch at the critical current of each branch. But the critical current I_c (or the return current I_r) for each branch is much different from each other. The IV curve for 8-min etching shows similar behavior to that for $t_e = 6.5$ min, while the critical current in each branch reduced rapidly (not shown here). The significant discrepancy in I_c (or I_r) most likely resulted from the differences in the junction area for a series of IJ's near the bottom of a stack due to inhomogeneous etching around the boundary of a stack. The irregularity in the values of I_c and I_r appearing in the high-bias range in the initial etching stages is seen to continuously reduce, and both of the quantities approach stable values of their own in the low-bias range as t_e increases [see Figs. 4(b)–4(f)]. This behavior also implies that the branches with the irregular I_c and I_r correspond to incompletely developed junctions near the bottom of the stack. When the etching time is increased beyond 10 min, at least a few low-bias branches in the IV curves start showing almost the same critical currents ($I_c \sim 2.3 \pm 0.1 \text{ mA}$) and return currents ($I_r \sim 70 \pm 4 \text{ } \mu\text{A}$). Thus, a few small stacks are believed to develop fully for $t_e \geq 10$

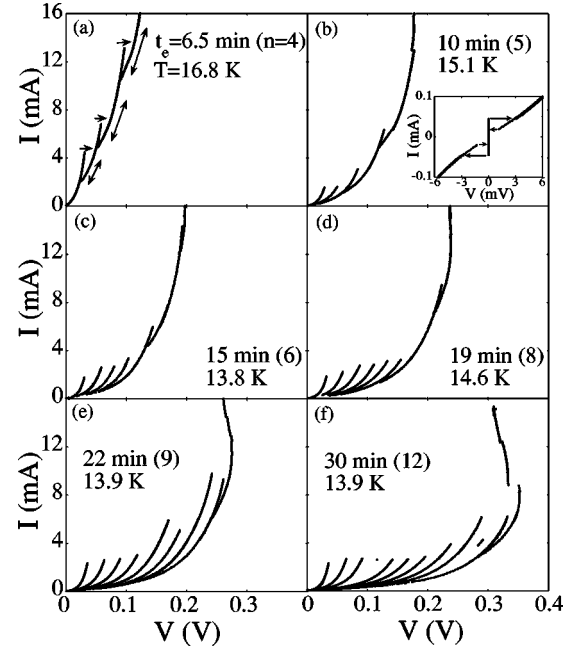


FIG. 4. Current-voltage characteristics for the etching time (a) $t_e = 6.5$ min ($n = 4$), (b) 10 min ($n = 5$), (c) 15 min ($n = 6$), (d) 19 min ($n = 8$), (e) 22 min ($n = 9$), and (f) 30 min ($n = 12$). The substrate temperatures were in the range 13.91–6.8 K. Inset: the enlarged view near zero bias that shows a hysteretic behavior of the surface WJ. Arrows indicate voltage changes while varying the bias current.

min. This conclusion is consistent with what we discussed in relation with the $R_c(T)$ curves.

If we consider the stack as a c -axis one-dimensional array of the underdamped Josephson junctions,^{42,43,53} the McCumber parameter⁵⁴ β_c deduced from the ratio⁵⁵ $I_r/I_c \sim 4/(\pi\sqrt{\beta_c}) \approx 0.031$ is about 1600, which is about two or three times larger than the results of others, i.e., $\beta_c = 500$ (Ref. 11) or 300–700 (Refs. 23 and 25). This difference may arise from a high critical current density $j_c \approx 1300 \text{ A/cm}^2$ of our sample. One should note that the first quasiparticle branch in the IV curves in three-probe measurements comes from the D'ID surface WJ. The magnified view of the first branch in a very low-bias range in the inset of Fig. 4(b) shows a hysteretic behavior with a much smaller critical current $I'_c = 46 \pm 3 \text{ } \mu\text{A}$ and return current $I'_r = 18 \pm 1 \text{ } \mu\text{A}$.

The negative dynamic resistance or the “backbending” for a set of longer etching times in Figs. 4(d)–4(f) is a generic feature in the IV characteristics of stacked tunneling Josephson junctions.⁵⁶ Either a nonequilibrium quasiparticle distribution in ultrathin conducting layer^{3,6} or a Joule heating effect⁵⁷ has been proposed to explain the feature. Figure 4 clearly demonstrates that the backbending develops gradually as the number of IJ's in the same stack increases, attributing it to a high-bias effect. In Fig. 5 we replotted the high-bias branches showing the backbending behavior for the different number of junctions in the stack. The backbending feature is visible, even from the early stages of etching ($t_e = 15$ min corresponding to $n = 6$), and becomes more pronounced for longer etching. A remarkable feature in this figure is that the voltage-turning points lie well on the 3-mW power-dissipation line. Although no symptom of temperature

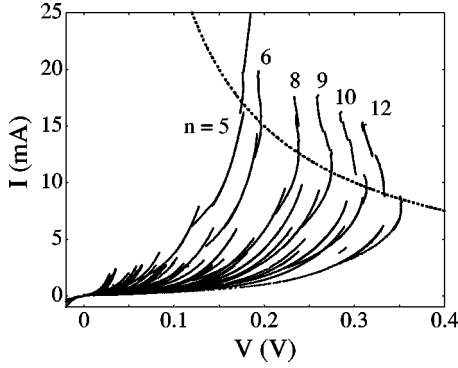


FIG. 5. A replot of the high-bias branches showing the backbending behavior in Fig. 4 for different numbers of junctions in the stack. The dotted line represents the 3-mW power line, which passes through the voltage-turning points of the curves, pointing toward the Joule-heating mechanism for the backbending behavior.

change was detected in the thermometry, this strongly suggests that Joule heating could be a likely cause of the backbending effect.

Careful examination of Fig. 5 reveals that as t_e increases a certain quasiparticle branch for a constant current bias shift to higher voltage range. This is opposite to what one would expect from the nonequilibrium quasiparticle distribution or from the Joule heating effect. We infer that it arises from the increase in the junction resistance R'_n and R_n due to shrinking of the junction area with increasing t_e .

In Fig. 6, we replotted the first low-bias branch of IV curve for $t_e=6.5$ min, which was already shown in Fig. 4(a), and the first three low-bias branches of six sets of IV curves corresponding to the etching times from 10 min to 30 min. To eliminate the variation of the junction resistance with t_e , the current axis in each IV curve was rescaled by multiplying $R_c(T_c)$ obtained from Fig. 2(a). One notices that in this rescaled plot the first branch of $t_e=6.5$ min almost coincides with the first stable branch for $t_e=10$ min or longer. The first stable branch arises from the surface WJ in D'ID configuration, and the second and third branches from the inner IJ's, both in DID configuration. If we assume that the D'ID (DID) junction has the same junction resistance R'_n (R'_n) as the N'ID (NID) junction, we can rewrite the IV relation for the WJ (primed variables) and IJ's (unprimed variables) as follows:

$$I_{D'ID} \times R_n' = \frac{1}{e} \int_{-\infty}^{\infty} N'(E; \Delta') N(E+eV; \Delta) [f(E) - f(E+eV)] dE, \quad (3)$$

in which Δ' is the temperature-dependent suppressed energy gap of the surface layer. Both R'_n and R_n contain the possible variation of the junction area with etching times. Equation (3) predicts that each IV curve of the WJ or a IJ will show its own scaling behavior with respect to different junction resistances R'_n and R_n , depending only on the energy gap Δ' and Δ . The remarkable feature in Fig. 6 is that, when scaled by $R_c(T_c)$ all together, all the three branches, for significantly different etching times longer than 10 min, fall into three merging curves. This confirms a definite proportionality ex-

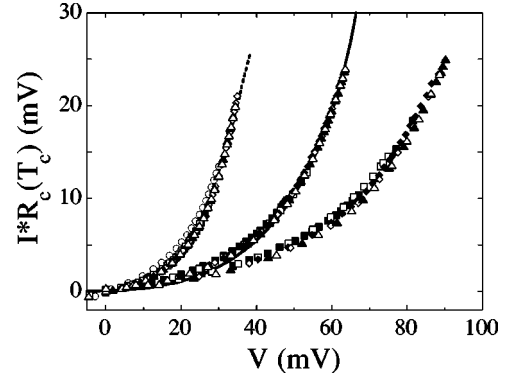


FIG. 6. Replot of the first low-bias branch of IV curve for $t_e=6.5$ (open circle) minutes shown in Fig. 4(a), together with the first three low-bias branches of 6 sets of IV curves corresponding to the etching times of 10 (solid square), 12 (open square), 19 (solid diamond), 22 (open diamond), 26 (solid triangle), and 30 (open triangle) minutes. The symbols are not clearly identifiable because of the high overlap of the data. The dotted line in the first branch (the solid line in the second branch) is the fit to the behavior of D'ID surface WJ (a DID inner IJ). The specimen temperatures were in the range 13.9–16.8 K.

isting between R'_n and R_n , regardless of the etching time t_e . The point will become clearer in the discussion in relation with Fig. 7(a) below.

We now determine the value of the zero-temperature energy gap in the surface layer, Δ'_0 , by fitting the first stable branch to Eq. (3), while adopting $\Delta_0=32.6$ meV, which was already obtained from the fit of $R_c(T)$ in Fig. 2(b), and setting R'_n to be $R_c(T_c)$ obtained from Fig. 2(a). The best-fit value⁵⁸ is $\Delta'_0=15.3 \pm 1.1$ meV assuming the BCS temperature dependence of gap energy with $\alpha=1.45$. This value of the surface gap is about one-half of the intrinsic gap value for any number of fully developed junctions. From the best fit of the second or the third branch to Eq. (3), we obtain $R_n=1.54 \Omega$ for $t_e=30$ min, which is about one sixth of $R'_n(30 \text{ min})=R_c(T_c; 30 \text{ min})$. It yields the characteristic voltage $I_c R_n \approx 3.5$ mV, which is much smaller than $\pi \Delta_0/2e=51.2$ mV predicted by the Ambegaokar-Baratoff relation⁵⁹ in conventional superconductors or the theoretical prediction Δ_0/e for $d_{x^2-y^2}$ symmetry.⁶⁰ The value $R_n=1.54 \Omega$ corresponds to $\rho_n \approx 23 \Omega \text{ cm}$, which is close to the value of $\rho_{c, \text{single}} \approx 20-22 \Omega \text{ cm}$ of IJ's in the high-temperature region (see Fig. 3). Thus the enhanced R_c above R_n around $T_{c, \text{onset}}$ is believed to be the quasiparticle contribution discussed in Ref. 6.

Since junctions in a stack switch to the higher resistive state before reaching the gap edge of a junction, there are uncertainties in determining both the normal-state resistance R_n and the critical current I_c directly from the data. As pointed out in Ref. 9, in a fit to Eq. (3) the values of R_n and Δ_0 are interrelated. For instance, one gets the smaller fit value of R_n for the choice of larger Δ_0 . We eliminated this uncertainty by adopting the measured values of $R_c(T_c)$ for R'_n , and alternatively determined Δ_0 , Δ'_0 , and R_n , respectively, from the normalized $R_c(T)$ curves in Region II and IV curves in Region I. This process is possible only for repeated progressive measurements in a single piece of crystal with the same material parameters Δ'_0 and Δ_0 through the entire measurements.

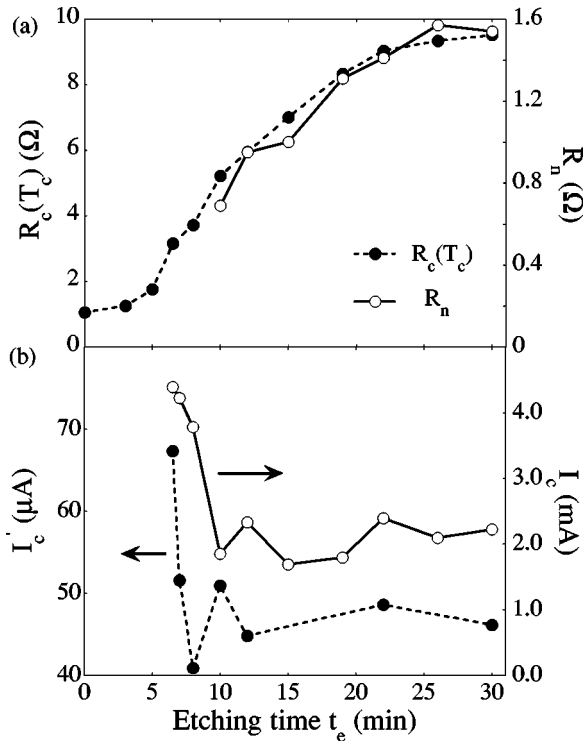


FIG. 7. (a) The etching time dependence of $R_c(T_c)$ obtained from Fig. 2(a) and the normal-state resistance R_n obtained from the numerical fit to Eq. (3) of the IV curves for the second branches in Fig. 6 below T_c' . For comparison the resistance values were normalized by those for $t_e=30$ min; $R_c(T_c)=9.52 \Omega$ and $R_n=1.54 \Omega$. The lines are guides to the eyes. (b) The etching time dependences of I_c and I_c' at $T=13-16$ K. The critical currents were taken from the first (I_c') and the second (I_c) quasiparticle branches of the IV curves below T_c' as shown in Fig. 4. The lines are guides to the eyes.

The consistency of the above fits are further ascertained by cross-checking the etching time dependence of the junction parameters obtained by different methods. In Fig. 7(a) we plot R_n determined from a fit of the second branch to Eq. (3) for different etching times of $t_e=10-30$ min. We also plotted $R_c(T_c)$ obtained directly from Fig. 2(a) for different t_e . Although showing a large difference in the absolute values for a given t_e , the two data sets obtained by different ways, when normalized by the values at $t_e=30$ min, i.e., $R_c(T_c; 30 \text{ min}) \equiv R_n'(30 \text{ min})=9.52 \Omega$ and $R_n(30 \text{ min})=1.54 \Omega$, show an excellent agreement with one another for all the ranges of t_e values. This fact makes it clearer that a definite proportionality exists between R_n' and R_n in any stack-forming etching stages. The value of $R_c(T_c)$ starts increasing for $t_e>5$ min and becomes fully stabilized for t_e around 19 min. The minimal etching time required for the full development of the stack can also be examined from the t_e dependence of the critical currents⁶¹ I_c' of the WJ and I_c of IJ's as shown in Fig. 7(b). The critical currents were taken from the first (I_c') and the second (I_c) quasiparticle branches of the IV curves in Fig. 4. Both values of I_c' and I_c are stabilized for t_e around 10–15 min.

IV. CONCLUSIONS

In this study, we focused on the evolution of the tunneling characteristics for stacks containing a few intrinsic junctions,

for temperatures above and below the bulk superconducting transition temperature of Bi-2212 single crystals. Three-probe measurements in comparison with usual four-probe measurements provided an advantage of enabling us to investigate the nature of the surface junction with suppressed coupling strength as well as the conducting properties of the inner junctions. Compared with a previous attempt by others,⁸ we were capable of lowering temperatures even below the Josephson coupling temperature T_c' of the surface junction using liquid-helium cooling. Our study reveals that $R_c(T)$ curves are scaled by the junction resistance of the surface WJ below T_c' . On the other hand, the IV characteristics for both IJ's and the WJ in stable etching stage for $t_e \geq 6.5$ min are scaled by the junction resistance of WJ, which indicates that a definite proportionality exists between the values of junction resistances of the WJ and IJ's.

One of the main findings of this study is that the gap in the surface layer Δ_0' is much reduced from the bulk value of IJ's, while the junction resistance of the surface WJ (R_n') is much larger than that of the IJ's (R_n). We obtained R_n from a fit to the second IV branch as shown in Fig. 6. Mentioned earlier, in a fit to Eq. (3) an almost similar fit quality can be achieved by choosing different values for interrelated parameters R_n and Δ_0 . Instead of obtaining R_n' from $R_c(T_c)$, just setting R_n' to be R_n , for example, may be a reasonable choice. With this choice, however, the fit gives $\Delta_0' \geq 3\Delta_0$, i.e., the surface layer has a gap about three times larger than the inner layers. Recently it has been claimed that, in the underdoped regime, the gap Δ_0' has a larger value^{34-36,62} even for a lower transition temperature T_c' . Thus it may seem plausible to expect widening of the gap at the surface layer while T_c' is suppressed. However, the universal relation between the superconducting gap and the transition temperature in Ref. 35 indicates that the magnitude of the gap for $T_c' \approx 30$ K is at best $\Delta_0' \sim 1.3\Delta_0$, which is far smaller than $3\Delta_0$ obtained from the fit above. In addition, it has also been known that the suppression of the transition temperature of Bi-2212 material itself down to 17–36 K cannot be achieved with a high degree of oxygen deficiency, because a band with Bi-O antibonding near the Fermi level acts as a source of holes.⁶³ The picture that the surface layer is more underdoped than the inner layers is again contradictory to the behavior revealed in Fig. 3, where the opposite was concluded earlier. In this sense, we discard the picture of an increased gap with suppressed transition temperature at the surface layer, and cling to the original results of fit with a suppressed surface gap. In this case, however, we must provide an explanation for the concurrent reduction of T_c' and Δ_0' in the surface layer, which is apparently in contradiction to the known relation³⁵ between the two variables. The only way to eliminate the inconsistency is to assume that the concurrent suppression of Δ_0' and T_c' of the surface layer is not caused by the change in the doping level in it, but by its proximity contact to the Au normal electrode as supposed by us in Ref. 11. Recently, Manabe and co-workers observed that, in scanning tunneling spectroscopy measurements on Bi-2212, the gap becomes smaller as the tip approaches closer to the crystal surface.³³ We believe this is consistent with our claim of the proximity-induced suppression of the gap on the surface layer in our specimen. Although currently, to our knowledge,

no theory is available to allow any quantitative confirmation of our claim, this study apparently strengthens our previous arguments.

Recently there have been tunneling spectroscopic studies on the nature of order-parameter symmetry of $\text{YBa}_2\text{Cu}_3\text{O}_{6+\delta}$ (YBCO-123) and Bi-2212 superconducting materials by employing high- T_c superconductor/normal metal/conventional s -wave superconductor hybrid junctions.^{29,44,45} Some of these studies have reported the existence of significant and finite s -wave components for YBCO-123 and Bi-2212 superconducting materials, respectively.^{29,45} Our study indicates that in tunneling spectroscopy using the above-mentioned hybrid junctions one should be concerned about the change in the superconducting state at the crystal surface, not by the oxygen deficiency as one might easily assume, but by the contact of $d_{x^2-y^2}$ -wave surface layers with a normal layer in a junction. On the other hand, scanning tunneling spectroscopy may be more affected by the oxygen deficiency at the surface.

The variation of the junction area along with continuous etching, in fact, acts as a disadvantage in studying the inherent tunneling properties in the system. Ironically, however, this can be advantageous as in this study, because as illustrated both in Fig. 2 and in Fig. 6, we were able to be convinced that, once the data are normalized by proper area-dependent parameters like junction resistance, the junctions in any etching stage exhibit no discernible variation in their properties, regardless of the number of junctions contained.

This leads us to the conclusion that not much correlation effect is present among the IJ's. Material parameters such as Δ'_0 and Δ_0 do not change in the whole *in situ* etching/measurements process, which thus gives stronger conviction of the scaling behavior in our $R_c(T)$ and IV data as discussed above.

The *in situ* technique is also extremely useful to study the so-called backbending effect. It convinces one that the effect develops by increasing the number of junctions contained in a single piece of crystal, which in turn allows us to draw a power-dissipation line. Comparing the backbending feature in the IV branches from different crystals in terms of power dissipation would be less meaningful. This technique is expected to provide powerful means to examine both the inter-layer coupling properties in the superconducting state and the in-plane conducting nature in the normal state.

ACKNOWLEDGMENTS

We wish to acknowledge useful discussions with Professor M. Tachiki. We are grateful to Professor M. Oda for providing valuable information on his recent work on the doping-level dependence of the pseudogap behavior. This work was supported by the Korea Science and Engineering Foundation under Contract No. K97005, Basic Science Research Institute funded by the Ministry of Education and POSTECH under Contract No. INH9825602, and the Ministry of Defense through MARC.

-
- ¹For recent works, see *Proceedings of the First RIEC International Symposium on Intrinsic Josephson Effects and THz Plasma Oscillations in High- T_c Superconductors, Sendai, Japan* [Physica C **293** (1997)].
- ²R. Kleiner, F. Steinmeyer, G. Kunkel, and P. Müller, Phys. Rev. Lett. **68**, 2394 (1992); R. Kleiner and P. Müller, Phys. Rev. B **49**, 1327 (1994).
- ³K. Tanabe, Y. Hidaka, S. Karimoto, and M. Suzuki, Phys. Rev. B **53**, 9348 (1996); M. Itoh, S. Karimoto, K. Namekawa, and M. Suzuki, *ibid.* **55**, R12 001 (1997).
- ⁴J. Takeya, S. Akita, J. Shimoyama, and K. Kishio, Physica C **261**, 21 (1996).
- ⁵A. Yurgens, D. Winkler, N. V. Zavaritsky, and T. Claeson, *Proceedings of Oxide Superconductors: Physics and Nanoengineering II, San Jose, CA* (SPIE, Bellingham, 1996), Vol. 2697, pp. 433–442.
- ⁶A. Yurgens, D. Winkler, N. V. Zavaritsky, and T. Claeson, Phys. Rev. B **53**, R8887 (1996); Phys. Rev. Lett. **79**, 5122 (1997).
- ⁷K. Schlenga, G. Hechtfisher, R. Kleiner, W. Walkenhorst, P. Müller, H. L. Johnson, M. Veith, W. Brodkorb, and E. Seibeiss, Phys. Rev. Lett. **76**, 4943 (1996).
- ⁸A. Yurgens, D. Winkler, T. Claeson, and N. V. Zavaritsky, Appl. Phys. Lett. **70**, 1760 (1997); Physica C **293**, 181 (1997).
- ⁹K. Schlenga, R. Kleiner, G. Hechtfisher, M. Mößle, S. Schmitt, P. Müller, Ch. Helm, Ch. Preis, F. Forsthofer, J. Keller, H. L. Johnson, M. Veith, and E. Steinbeiß, Phys. Rev. B **57**, 14 518 (1998).
- ¹⁰A. Odagawa, K. Setsune, M. Sakai, and H. Adachi, Jpn. J. Appl. Phys., Part 1 **37**, 486 (1998).
- ¹¹N. Kim, Y.-J. Doh, H.-S. Chang, and H.-J. Lee, Phys. Rev. B **59**, 14 639 (1999).
- ¹²S.-J. Kim, Yu. I. Latyshev, and T. Yamashita, Appl. Phys. Lett. **74**, 1156 (1999); Yu. I. Latyshev, S.-J. Kim, and T. Yamashita, Pis'ma Zh. Eksp. Teor. Fiz. **69**, 75 (1999) [JETP Lett. **69**, 84 (1999)].
- ¹³J. H. Cho, M. P. Maley, S. Fleshler, A. Lacerda, and L. N. Bulaevskii, Phys. Rev. B **50**, 6493 (1994); S. Luo, G. Yang, and C. E. Gough, *ibid.* **51**, 6655 (1995).
- ¹⁴T. Yasuda, R. Kondo, S. Takano, T. Fukami, and T. Aomine, Physica C **263**, 416 (1996).
- ¹⁵Yu. I. Latyshev, J. E. Nevelskaya, and P. Monceau, Phys. Rev. Lett. **77**, 932 (1996).
- ¹⁶N. Mros, V. M. Krasnov, A. Yurgens, D. Winkler, and T. Claeson, Phys. Rev. B **57**, R8135 (1998); G. Yu. Logvenov, M. V. Fistul, and P. Müller, *ibid.* **59**, 4524 (1999).
- ¹⁷M. Suzuki, T. Watanabe, and A. Matsuda, Phys. Rev. Lett. **81**, 4248 (1998).
- ¹⁸A. Yurgens, D. Winkler, T. Claeson, G. Yang, I. F. G. Parker, and C. E. Gough, Phys. Rev. B **59**, 7196 (1999).
- ¹⁹R. Kleiner, P. Müller, H. Kohlstedt, N. F. Pedersen, and S. Sakai, Phys. Rev. B **50**, 3942 (1994).
- ²⁰J. U. Lee, J. E. Nordman, and G. Hohenwarter, Appl. Phys. Lett. **67**, 1471 (1995); J. U. Lee, P. Guptasarma, D. Hornbaker, A. El-Kortas, D. Hinks, and K. E. Gray, *ibid.* **71**, 1412 (1997).
- ²¹G. Hechtfisher, R. Kleiner, K. Schlenga, W. Walkenhorst, P. Müller, and H. L. Johnson, Phys. Rev. B **55**, 14 638 (1997).
- ²²V. M. Krasnov, N. Mros, A. Yurgens, and D. Winkler, Phys. Rev. B **59**, 8463 (1999).

- ²³A. Irie, Y. Hirai, and G. Oya, *Appl. Phys. Lett.* **72**, 2159 (1998).
- ²⁴A. Irie and G. Oya, *Physica C* **293**, 249 (1997); W. Prusseit, M. Rapp, K. Hirata, and T. Mochiku, *ibid.* **293**, 25 (1997).
- ²⁵H. L. Johnson, G. Hechtfisher, G. Gotz, R. Kleiner, and P. Müller, *J. Appl. Phys.* **82**, 756 (1997).
- ²⁶Y.-J. Doh, J. Kim, K.-T. Kim, and H.-J. Lee, *cond-mat/9908459* (unpublished).
- ²⁷G. Hechtfisher, R. Kleiner, A. V. Ustinov, and P. Müller, *Phys. Rev. Lett.* **79**, 1365 (1997).
- ²⁸M. Suzuki, S. Karimoto, and K. Namekawa, *J. Phys. Soc. Jpn.* **67**, 732 (1998); A. Yurgens, D. Winkler, T. Claeson, S.-J. Hwang, and J.-H. Choy, *cond-mat/9907159*, *Int. J. Mod. Phys. B* (to be published).
- ²⁹M. Mössle and R. Kleiner, *Phys. Rev. B* **59**, 4486 (1999).
- ³⁰H. J. Tao, A. Chang, F. Lu, and E. L. Wolf, *Phys. Rev. B* **45**, 10 622 (1992); E. L. Wolf, A. Chang, Z. Y. Rong, Yu. M. Ivanchenko, and F. Lu, *J. Supercond.* **7**, 355 (1994); L. Ozyuzer, Z. Yusof, J. F. Zasadzinski, R. Mogilevsky, D. G. Hinks, and K. E. Gray, *Phys. Rev. B* **57**, R3245 (1998).
- ³¹T. Matsumoto, S. Choopun, and T. Kawai, *Phys. Rev. B* **52**, 591 (1995).
- ³²Ch. Renner and Ø. Fischer, *Phys. Rev. B* **51**, 9208 (1995).
- ³³M. Oda, C. Manabe, and M. Ido, *Phys. Rev. B* **53**, 2253 (1996); C. Manabe, M. Oda, and M. Ido, *J. Phys. Soc. Jpn.* **66**, 1776 (1997).
- ³⁴Ch. Renner, B. Revaz, J.-Y. Genoud, K. Kadowaki, and Ø. Fischer, *Phys. Rev. Lett.* **80**, 149 (1998); Y. DeWilde, N. Miyakawa, P. Guptasarma, M. Iavarone, L. Ozyuzer, J. F. Zasadzinski, P. Romano, D. G. Hinks, C. Kendziora, G. W. Crabtree, and K. E. Gray, *ibid.* **80**, 153 (1998).
- ³⁵M. Oda, K. Hoya, R. Kubota, C. Manabe, N. Momono, T. Nakano, and M. Ido, *Physica C* **281**, 135 (1997); T. Nakano, N. Momono, M. Oda, and M. Ido, *J. Phys. Soc. Jpn.* **67**, 2622 (1998).
- ³⁶N. Miyakawa, P. Guptasarma, J. F. Zasadzinski, D. G. Hinks, and K. E. Gray, *Phys. Rev. Lett.* **80**, 157 (1998).
- ³⁷Y. Li, J. L. Huang, and C. M. Lieber, *Phys. Rev. Lett.* **68**, 3240 (1992).
- ³⁸H. Ding, T. Yokoya, J. C. Campuzano, T. Takahashi, M. Randeria, M. R. Norman, T. Mochiku, K. Kadowaki, and J. Giapintzakis, *Nature (London)* **382**, 51 (1996); Z.-X. Shen and J. R. Schrieffer, *Phys. Rev. Lett.* **78**, 1771 (1997).
- ³⁹A. V. Fedorov, T. Valla, P. D. Johnson, Q. Li, G. D. Gu, N. Koshizuka, *Phys. Rev. Lett.* **82**, 2179 (1999).
- ⁴⁰K. Takenaka, K. Mizuhashi, H. Takagi, and S. Uchida, *Phys. Rev. B* **50**, 6534 (1994); X. H. Chen, M. Yu, K. Q. Ruan, S. Y. Li, Z. Gui, G. C. Zhang, and L. Z. Cao, *ibid.* **58**, 14 219 (1998).
- ⁴¹T. Watanabe, T. Fujii, and A. Matsuda, *Phys. Rev. Lett.* **79**, 2113 (1997).
- ⁴²R. Kleiner, *Phys. Rev. B* **50**, 6919 (1994).
- ⁴³T. Koyama and M. Tachiki, *Phys. Rev. B* **54**, 16 183 (1996); M. Machida, T. Koyama, and M. Tachiki, *Physica C* **300**, 55 (1998).
- ⁴⁴D. A. Wollman, D. J. Van Harlingen, W. C. Lee, D. M. Ginsberg, and A. J. Leggett, *Phys. Rev. Lett.* **71**, 2134 (1993); D. A. Wollman, D. J. Van Harlingen, J. Giapintzakis, and D. M. Ginsberg, *ibid.* **74**, 797 (1995); S. Sinha and K.-W. Ng, *ibid.* **80**, 1296 (1998); H. Z. Durusoy, D. Lew, L. Lombardo, A. Kapitulnik, T. H. Geballe, and M. R. Beasley, *Physica C* **266**, 253 (1996).
- ⁴⁵A. G. Sun, D. A. Gajewski, M. B. Maple, and R. C. Dynes, *Phys. Rev. Lett.* **72**, 2267 (1994); K. A. Kouznetsov, A. G. Sun, B. Chen, A. S. Katz, S. R. Bahcall, J. Clarke, R. C. Dynes, D. A. Gajewski, S. H. Han, M. B. Maple, J. Giapintzakis, J.-T. Kim, and D. M. Ginsberg, *ibid.* **79**, 3050 (1997).
- ⁴⁶S. H. Liu and R. A. Klemm, *Phys. Rev. Lett.* **73**, 1019 (1994); S. R. Bahcall, *ibid.* **76**, 3634 (1996); A. M. Martin and J. F. Annett, *Phys. Rev. B* **57**, 8709 (1998).
- ⁴⁷M. Chung, H.-S. Chang, Y.-J. Doh, and H.-J. Lee, *J. Korean Phys. Soc.* **31**, 384 (1997).
- ⁴⁸The base mesa was consequently covered with $\sim 9000\text{-\AA}$ -thick Au film. Deposition of a quite thick Au film was necessary to secure the electrical connection across the crystal boundary.
- ⁴⁹This second superconducting transition is not shown in Refs. 3 and 17, where the specimens were annealed after gold deposition.
- ⁵⁰H. Won and K. Maki, *Phys. Rev. B* **49**, 1397 (1994).
- ⁵¹J. H. Xu, J. L. Shen, J. H. Miller, Jr., and C. S. Ting, *Phys. Rev. Lett.* **73**, 2492 (1994).
- ⁵²M. Tinkham, *Introduction to Superconductivity* (McGraw-Hill, New York, 1996), Chap. 3.
- ⁵³Ch. Helm, Ch. Preis, F. Forsthofer, J. Keller, K. Schlenga, R. Kleiner, and P. Müller, *Phys. Rev. Lett.* **79**, 737 (1997).
- ⁵⁴D. E. McCumber, *J. Appl. Phys.* **39**, 3113 (1968).
- ⁵⁵K. K. Likharev, *Dynamics of Josephson Junctions and Circuits* (Gordon and Breach, Philadelphia, 1986), Chap. 4.
- ⁵⁶D. Winkler and T. Claeson, *Phys. Scr.* **32**, 317 (1985).
- ⁵⁷M. Suzuki and K. Tanabe, *Jpn. J. Appl. Phys., Part 2* **35**, L482 (1996).
- ⁵⁸In our previous work (Ref. 11) we used the relation $\Delta'_0 = \Delta_0 T'_c / T_c$ to estimate Δ'_0 . Since the relation between the gap and the transition temperature due to proximity contact of $d_{x^2-y^2}$ -wave superconductor to a normal metal is not known we believe the direct extraction of the value from the fit as used in this study has more relevance.
- ⁵⁹V. Ambegaokar and A. Baratoff, *Phys. Rev. Lett.* **10**, 486 (1963); **11**, 104 (1963).
- ⁶⁰Y. Tanaka and S. Kashiwaya, *Phys. Rev. B* **56**, 892 (1997).
- ⁶¹The critical current of the surface junction I'_c , due to its suppressed superconductivity, is always about an order of magnitude smaller than those of inner junctions I_c .
- ⁶²In this case the gap may correspond to the single-particle excitation gap suggested by G. Deutscher [*Nature (London)* **397**, 221 (1999)].
- ⁶³A. Q. Pham, F. Studer, N. Merrien, A. Maignan, C. Michel, and B. Raveau, *Phys. Rev. B* **48**, 1249 (1993); P. Ghigna, G. Spinolo, G. Flor, and N. Morgante, *ibid.* **57**, 13 426 (1998).